

Learning to Predict Blood Pressure with Deep Bidirectional LSTM Network

Peng Su

PSU@EE.CUHK.EDU.HK

*Department of Electronic Engineering
The Chinese University of Hong Kong
Shatin, N.T. , Hong Kong*

Xiaorong Ding

XRDING@EE.CUHK.EDU.HK

*Department of Electronic Engineering
The Chinese University of Hong Kong
Shatin, N.T. , Hong Kong*

Yuanting Zhang

YTZHANGAPPLE@ICLOUD.COM

*Department of Electronic Engineering
The Chinese University of Hong Kong
Shatin, N.T. , Hong Kong*

Fen Miao

FEN.MIAO@SIAT.AC.CN

*Shenzhen Institutes of Advanced Technology
Chinese Academy of Sciences
Shenzhen, Guangdong, China*

Ni Zhao

NZHAO@EE.CUHK.EDU.HK

*Department of Electronic Engineering
The Chinese University of Hong Kong
Shatin, N.T. , Hong Kong*

Abstract

Blood pressure (BP) ¹ has been a difficult vascular risk factor to measure precisely and continuously due to its multiscale temporal dependencies. However, both pulse transit time (PTT) model and regression model fail to learn such dependencies and thus suffer from accuracy decay over time. In this work, we addressed the limitation of existing BP prediction models by formulating BP extraction as a sequence prediction problem in which both the input and target are temporal sequence. By incorporating both a bidirectional layer structure and a deep architecture in a standard long short term-memory (LSTM), we established a deep bidirectional LSTM (DB-LSTM) network that can adaptively discover the latent structures of different timescales in BP sequences and automatically learn such multiscale dependencies. We evaluated our proposed model on a static and follow-up continuous BP dataset, and the results show that DB-LSTM network can effectively learn different timescale dependencies in the BP sequences and advances the state-of-the-art by achieving superior accuracy performance than other leading methods on both datasets. To the best of our knowledge, this is the first study to validate the ability of recurrent neural networks to learn the multiscale dependencies of long-term continuous BP sequence.

1. BP in this paper refers to arterial blood pressure.

1. Introduction

Around 3 in 10 deaths globally are caused by cardiovascular diseases (CVD) - diseases of the heart and blood vessels that can cause heart attacks and stroke.² As the leading risk factor of CVD (Lim et al., 2013), high blood pressure (BP) has been commonly used as the critical criteria for diagnosing and preventing CVD. High BP, which is also known as hypertension, normally develops without obvious symptoms at early stage, making it a “silent killer”. Therefore, accurate and continuous BP monitoring during people’s daily live is extremely imperative for CVD prevention and diagnosis. In addition, blood pressure variability (BPV) reflects how a cardiovascular system regularize itself and response to external stimulus, and is another critical cardiovascular indicator that can only be obtained through continuous and long-duration BP monitoring.

Current BP measurement devices, e.g., Omron products, are cuff-based and therefore bulky, discomfort to wear, and only suitable for snapshot measurements. These disadvantages restrict the use of the cuff-based devices for continuous and frequent BP measurement, which are essential for nighttime monitoring and precise diagnosis of different CVD symptoms. Recent advancements in sensing technologies provide a wearable sensor network solution that can achieve cuffless and continuous BP monitoring (Chan et al., 2007; Zheng et al., 2014). These new emerged sensing technologies can detect several human physiological signs through contacting corresponding sensors to the human body. For example, electrocardiography (ECG) sensor can detect tiny skin impedance variations that arise from the hearts electrophysiologic pattern during each heart beat; photoplethysmogram (PPG) sensor can probe blood volume variation inside arteries, and etc. While all these physiological sensing signals contain enormous information of the functionality and health status of our cardiovascular system, the data is difficult to mine effectively due to noisy observation, missing value and varying length. Extensive research efforts have been made to develop effective models to predict or estimate BP from the sensor output; examples include the well established physiological modeling method - Pulse transit time model, and the recently proposed machine learning approach - regression model such as support vector machine, decision tree and etc.

Pulse transit time (PTT) model, a classic physiological model, has been seen as the most effective solution to realize continuous and unobtrusive BP measurement, and it was once the state-of-the-art model. The model builds a set of differential equations to describe the fluid dynamics inside our cardiovascular system (Nichols et al., 2011). With some specific assumptions and boundary conditions, a concise solution of the model equations can be obtained, based on which, a BP value can be calculated. Despite the simplicity of the PTT method, it fails to maintain the prediction accuracy over time, i.e., it can only keep its BP prediction accuracy within a short period of time (McCarthy et al., 2013). Accordingly, PTT method demands frequent calibration to maintain reliable estimation accuracy.

Since the relationship between input (e.g., ECG and PPG features) and output (BP) is much complex than the PTT model can describe, there have been attempts to apply supervised learning to mine the input-output function. This data-driven approach utilize a large number of training samples $\{x_i, y_i\}$ to train a regression model to learn the relationship between x and y . Here x_i denote the input variables, i.e. ECG, PPG and their derived

2. WHO 2014, http://www.who.int/features/factfiles/global_burden/en/

features, and y_i denote the target variable that we are interested in, i.e. BP. However, the simple regression models still don't have the ability to approximate the complex function of BP dynamic system.

In this paper, we propose a novel recurrent neural networks (RNNs), which can effectively learn the multi-timescale dependencies from a sequential BP data. The model, which is referred as *deep bidirectional long short-term memory network* (DB-LSTM), does not require explicit pre-processing or transformation of input sequence, but adaptively discover the latent structures of different timescales and automatically learn the multiscale dependencies. In our approach, a task is formulated as a temporal sequence predicting problem that can be solved under sequence-to-sequence learning framework. Firstly, we build a LSTM network that incorporates with a bidirectional structure, enabling each neuron to access longer range context in both the past and future directions and thus making the model more sensitive to the sequence variation patterns. Secondly, considering existence of multi-timescale dependencies in the BP sequence, we extend the *bidirectional LSTM* to *deep bidirectional LSTM* by stacking multiple *bidirectional LSTM* modules to learn the hierarchical representation for different timescale dependencies. We evaluate this model on two datasets: static and follow-up continuous BP dataset. The results on static continuous BP dataset demonstrate that DB-LSTM outperform the conventional pulse transit time (PTT) model, regression model and vanilla *LSTM*. On follow-up continuous BP dataset, the DB-LSTM also achieves the state-of-the-art accuracy performance comparing with all the other methods. To our best knowledge, this is the first work to explore the capability of RNN in predicting long-term (e.g., multi-day) continuous blood pressure.

The key contributions of this work are as follows:

- We demonstrate for the first time that an RNN model is capable of learning the latent structures of different timescales in a long-term (e.g., multi-day) continuous BP sequence.
- We propose a novel *RNN* called *deep bidirectional long short-term memory network* to effectively learn the multi-timescale dependencies in a continuous BP sequence.
- We have achieved a new benchmark for both multi-day and static continuous BP prediction accuracy.

2. Related Work

Existing methods for BP prediction can roughly be categorized into two groups, namely physiological modeling that relies on our domain knowledge to analytically derive BP values, and data-driven approach that applies machine learning techniques to learn the relationship between input and target (i.e., BP). In the following we will first introduce a physiological modeling approach, pulse transit time model, and then describe two data driven approaches, regression model and recurrent neural networks.

Pulse Transit Time Model (PTT) was first proposed by Weltman et al. (1964). It works on the principle of pulse wave velocity (PWV) through the Moens-Korteweg equation $PWV = \sqrt{Eh/2\rho R}$ which is the approximate solution of hemodynamics differential equations. This equation depict the relationship tween PWV and artery elastic modulus E

under the constant assumption of thickness h to artery radius R ratio, where E was found empirically to be exponentially related with BP by Hughes et al. (1979). In practice, people use PTT which can be derived from the time interval between ECG R peak and the characteristic PPG point to calculate PWV through $PWV = L/PTT$ by assuming that the distance between heart and peripheral site L is constant. Finally we can obtain the function $BP = f(PTT)$ that can be used to estimate BP. However, there is a series key underlying assumptions may not be true in real situation, like assume arterial radius, artery thickness, blood density and viscosity all are constant, etc (Nichols et al., 2011). In order to find optimal f , lots of researchers have try to extract more informative features that may regulate or relate to some parameters inside PTT model from ECG, PPG and other related physiological data (Li et al., 2014; Ding and Zhang, 2014). In addition, the most important assumption underlying PTT model is that it assumes all the BP data at different time are independent with each other. This assumption significantly limits the ability of the PTT model to process BP sequence.

Regression Model. The BP prediction task can be formulated as a regression problem that given input of ECG, PPG and their derived features x_t to predict our target output BP y_t by modeling $P(y_t | x_t)$. These method normally consist of two stages : the first stage is to learn data representation which also know as feature extraction or feature engineering, the second stage is to learn the parameters of task-specific regression model. Regression model theory has been well developed by machine learning community. Typical regression methods include linear regression, support vector regression, decision tree, etc. Most of recent research focus on manually designing effective data representation or features based on our domain knowledge (Kachuee et al., 2015; Monte-Moreno, 2011; Li et al., 2014). This approach in principle has more capability to model the complex problem settings because it can absorb much a larger variety of information as one design more input features. However, the regression model holds the same independent and identically distributed (i.i.d.) assumptions on training samples as the PTT model, which impair its ability for modeling sequential data.

Recurrent Neural Networks. Recurrent Neural Networks or RNNs (Rumelhart et al., 1985) are a family of neural networks for processing sequential data. While RNNs have a long history of successful applications in various sequence learning tasks (Rumelhart et al., 1985; Werbos, 1988; Hochreiter and Schmidhuber, 1997), the challenge of effectively learning long-term dependencies (Goodfellow et al., 2016) has encouraged various research efforts for improving the RNN architecture. Among the most successful RNN variants are the Long Short Term Memory networks (Hochreiter and Schmidhuber, 1997), which have been proven to be extremely effective model in a wide range of machine learning applications that involve sequential data such as speech recognition (Graves et al., 2013), machine translation (Sutskever et al., 2011), language modeling (Mikolov et al., 2010), video analysis (Donahue et al., 2015) and image captioning (Vinyals et al., 2015). RNNs have also been applied to study health data (Che et al., 2016; Choi et al., 2015, 2016; Lipton et al., 2015, 2016; Silipo and Marchesi, 1998), however, most of these applications focus on classification tasks, such as diagnosis classification based on Electronic Health Record (Lipton et al., 2015), ECG analysis (Silipo and Marchesi, 1998), seizure detection based on EEG (Thodoroff et al., 2016), etc. The potential of LSTM to predict multi-day BP from multivariate physiological signals remains to be unexplored.

3. Problem Formulation and Analysis

The goal of BP prediction is to use multi sequential physiological signal to predict BP sequence. Suppose we observe multi physiological data denoted as $(x_1, x_2 \dots, x_T)$, where $x_t \in \mathbb{R}^M$ represents the t -th observations of all M input variables (e.g., ECG and PPG features). Let $(y_1, y_2 \dots, y_T)$ denote the blood pressure (BP) sequence that we want to predict. Systolic blood pressure (SBP) and diastolic blood pressure (DBP) are the two most frequently used BP indicators. So here we use y_t to denote a vector $[SBP, DBP]$ at time step t .

For PTT model, it assumes that BP at different time steps are independent with each other like Equation.1 depict.

$$p(y_1, \dots, y_T \mid x_1, \dots, x_T) = \prod_{t=1}^T p(y_t \mid x_t) \quad (1)$$

Here the PTT method describes the hemodynamics in a human body based on classical mechanical fluid dynamic models, but neglects the fact that the cardiovascular system is a complex dynamic system that involves multiple feedback control loops (Akselrod et al., 1985; Guyton et al., 1972; Nichols et al., 2011) which responds to BP variation (Akselrod et al., 1985). In other words, BP data at different time are coupled or related with its neighbors as shown in Equation.2.

$$p(y_1, \dots, y_T \mid x_1, \dots, x_T) = \prod_{t=1}^T p(y_t \mid x_t, x_{t-1}, \dots, x_1) \quad (2)$$

In particular, the feedback control mechanism plays a more important role than the fluid dynamic in long term BP fluctuation, as it maintains our physiological equilibrium. This is why the PTT model can not model intricate patterns of BP variation and thus suffers from long term BP estimation accuracy decay (McCarthy et al., 2013).

For regression model, the studies have so far assumed that a sequence of random variables are independent and identically distributed (i.i.d.) to simplify the underlying mathematics of sequence inference. In this regard, the regression model also shares the same drawback as the PTT model, which y_t at different time steps are independent with each other. Consequently, the i.i.d. assumption crucially weakens the ability of this model to process sequential data.

Based upon the above analysis, the model we proposed in this work rely on the non-i.i.d. prerequisite.

4. The Model

We now present our *deep bidirectional LSTM network* shown in Figure 1. Although *recurrent neural network* (RNN) (Rumelhart et al., 1985) and its variants *long short-term memory* (LSTM) (Hochreiter and Schmidhuber, 1997) have proven to be powerful dynamic systems for modeling sequential data (LeCun et al., 2015), they are still limited to learn the complex dependencies mixed by different timescales (El Hiji and Bengio, 1995). To address this problem, we first propose an extension of vanilla LSTM which has a bidirectional layer

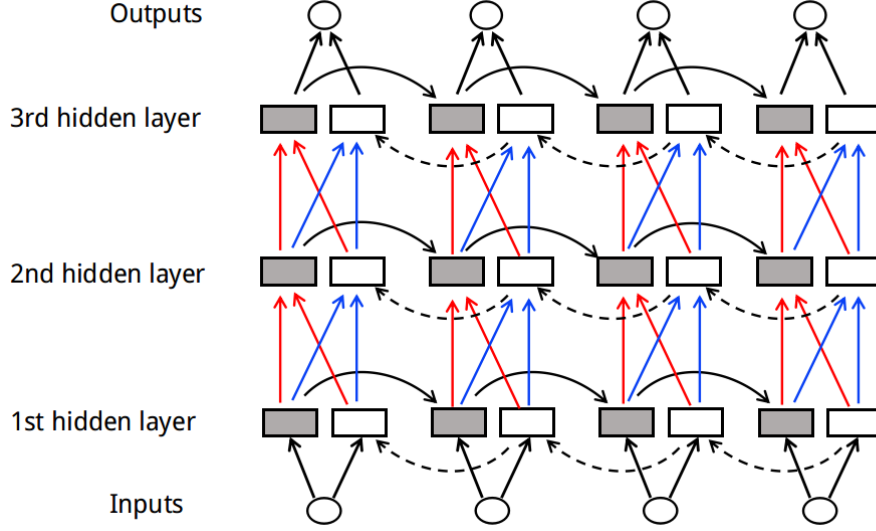


Figure 1: Deep Bidirectional LSTM architecture. The gray and white box represent forward hidden sequence and backward hidden sequence of each layer respectively. And both of them adopt LSTM cell structure.

structure that can absorb both the past and nearby future context information in sequential data. Secondly, by stacking multiple *bidirectional LSTM* layers to form a *deep bidirectional LSTM network*, we are able to disentangle the intricate mixing dependencies and learn the hierarchical representation for different timescale dependencies with multiple levels of abstraction.

Long short-term memory (LSTM) was designed to address the vanishing gradient problem of conventional *recurrent neural network* (RNN). In addition to a hidden state vector h_t , LSTM also incorporate a explicit memory cell c_t which can decide when to accumulate or forget the old state information by gating mechanism (see Figure 2). The precise form of update is as follows:

$$f_t = \sigma(W_f x_t + U_f c_{t-1} + b_f) \quad (3)$$

$$i_t = \sigma(W_i x_t + U_i c_{t-1} + b_i) \quad (4)$$

$$o_t = \sigma(W_o x_t + U_o c_{t-1} + b_o) \quad (5)$$

$$c_t = f_t \circ c_{t-1} + i_t \circ \sigma(W_c x_t + U_c c_{t-1} + b_c) \quad (6)$$

$$h_t = o_t \circ \tanh(c_t) \quad (7)$$

where f , i , o , and c are respectively the forget gate, input gate, output gate and cell state, σ denote the element-wise sigmoid function, and “ \circ ” denotes the Hadamard product.

4.1 Bidirectional LSTM Structure

In this section, we will present the single-layer learning modules of our model called *bidirectional LSTM* network. Conventional LSTM provide an elegant way to tackle sequence

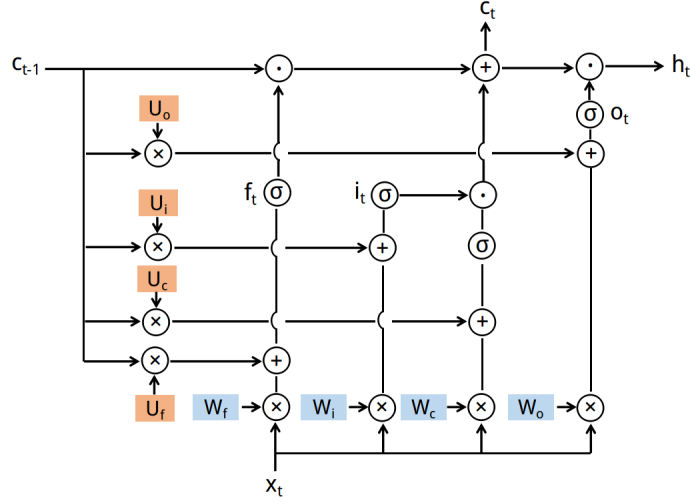


Figure 2: LSTM computing graph.

learning problem by a “causal” structure, meaning that the state at time t only captures information from the past, x_1, \dots, x_{t-1} , and the present input x_t . In a BP prediction problem, since our human cardiovascular system owns a closed-loop feedback regulation mechanism, BP at a time point is closely related to both its past and future states. In other words, future input information can also provide insight about hidden states that can help predicting BP. Bidirectional RNN (BRNN) (Schuster and Paliwal, 1997) can realize this function by processing the data in both directions with two separate hidden layers, which then merge to the same output layer. As illustrated in Figure. 3, a BRNN computed the forward hidden sequence h_t , the backward hidden sequence k_t and the output sequence y_t by updating the following equations:

$$h_t = \mathcal{F}(W_{hh}h_{t-1} + W_{xh}x_t + b_h) \quad (8)$$

$$k_t = \mathcal{F}(W_{kk}k_{t+1} + W_{xk}x_t + b_k) \quad (9)$$

$$y_t = g(W_{hy}h_t + W_{ky}k_t + b_y). \quad (10)$$

In our proposed model, all the hidden state vectors update function \mathcal{F} adopted in the LSTM formula, which means \mathcal{F} is implemented by composite Equation 3 to 7. This bidirectional LSTM allows the output units y_t to automatically learn a representation that depends on both the past and the future but is most sensitive to the input values around time t , without having to specify a fixed-size window around t (a regular RNN have to deal with a fixed-size look-ahead buffer). In addition to making the model more robust, the bidirectional structure also dramatically improves the model overall performance.

4.2 Deep Architecture

It is important to point out that BP sequences have not only temporal dependencies but also a multi-timescale structure. It has previously been found that human blood pressure

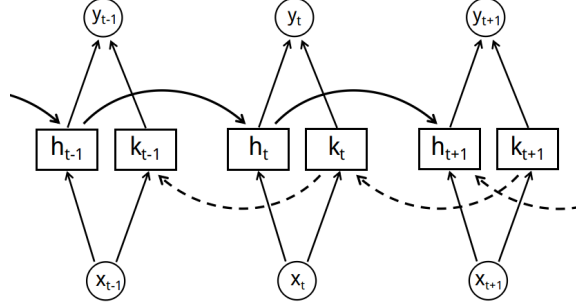


Figure 3: Bidirectional LSTM structure. h_t represent forward hidden sequence and k_t represent backward sequence. Hidden units designed by this way can implicitly contain abundant information about the history of all the past elements of the sequence.

(BP) mainly fluctuates at some specific time scales corresponding to high frequency (0.14-0.35 Hz), middle frequency (0.07-0.14 Hz) and low frequency (0.025-0.07 Hz) (Parati et al., 1990). Accordingly, we may take advantage of this prior knowledge to improve our model. Here we convert the observed BP variation from frequency domain to time domain, thus we can interpret the HF, MF and LF patterns as short-term, middle-term and long-term dependencies or variation patterns.

Inspired by the recent remarkable success of deep learning, which generally depends on learning hierarchical data representation with increasing level of abstraction (Krizhevsky et al., 2012; LeCun et al., 2015; Bengio et al., 2013). In addition, it has been observed that higher-level representation (hidden state) changes slowly while lower-level representation (hidden state) are more sensitive to precise time steps (El Hihi and Bengio, 1995). Accordingly we construct a multilayer stack of *bidirectional LSTM* modules to learn different timescale dependencies of BP sequence.

The deep structure can be created by stacking multiple RNN hidden layer on top of each other, with the output of previous hidden layer forming the input of the next. To construct a *deep bidirectional LSTM* (DB-LSTM) with L layers, the above state transition function are modified to following equations:

$$h_t^i = \mathcal{F}(W_{h^i h^i}^i h_{t-1}^i + W_{q^{i-1} h^i}^i q_t^{i-1} + b_h^i) \quad (11)$$

$$k_t^i = \mathcal{F}(W_{k^i k^i}^i k_{t+1}^i + W_{q^{i-1} k^i}^i q_t^{i-1} + b_k^i), \quad (12)$$

where i denote the different layer and \mathcal{F} is also implemented in LSTM formula as previous. Note that the lower layer hidden state output q_t^{i-1} become

$$q_t^{i-1} = g(W_{h^{i-1} y^{i-1}}^{i-1} h_t^{i-1} + W_{k^{i-1} y^{i-1}}^{i-1} k_t^{i-1} + b_y^{i-1}). \quad (13)$$

The reason for this architecture is twofold. First, the higher-level neurons (hidden state variable) have much larger receptive field (the region of the input sequence that influence the response of the neuron), meaning that they can focus on discovering longer dependencies (e.g., between two inputs remote from each other in time), while the lower-level neurons only have relative short range access of input sequence, namely in charge of detecting

local short term variation patterns. Second, the long-term dependencies can be disentangled into middle-term dependencies and the same applied on middle-term and short-term dependencies. In other words, we obtain the higher-level representation (e.g., long-term dependencies) by composing lower-level ones (e.g., middle-term or short-term dependencies). And deep network architecture has been proven to be able to learn such hierarchical data representation efficiently with multiple levels of abstraction (LeCun et al., 2015).

By iteratively computing the above equations from layer $i = 1$ to L and time steps $t = 1$ to T , we can obtain the final output y_t

$$y_t = g(W_{h^L y} h_t^L + W_{k^L y} k_t^L + b_y^L). \quad (14)$$

Up to this point, all the structure details inside our Deep Bidirectional LSTM network have been presented. As illustrated in Figure 1, our LSTM model incorporate with both bidirectional architecture and deep structure to jointly learn to predict SBP and DBP. And the training objective is to minimize the mean squared error (MSE) as follow:

$$\mathcal{L}(\{x_1, \dots, x_t\}, \{y_1, \dots, y_t\}) = \mathbb{E}_{(x,y) \in \mathcal{D}} \left[\sum_t \|\hat{y}_t - y_t\| \right], \quad (15)$$

where $\|\cdot\|$ denote L^2 norm, \mathcal{D} denote training dataset, \hat{y}_t denote BP prediction and y_t denote BP ground truth. By extending the standard *long short-term memory* (LSTM) network to incorporated with both bidirectional layer structure and deep architecture, our model has proved to able to learn effective data representations, namely can generalize across much wider scope of variation patterns.

5. Network Training

While deeper RNN architectures owns larger learning capability, it typically becomes more difficult to train due to overfitting. Despite of common dropout procedure, we also applied multitask training and supervised pretraining to address this challenge in this work.

5.1 Multitask training

Given that we also have mean blood pressure (MBP) labels in our training dataset, and SBP, DBP and MBP are closely related to each other, this auxiliary domain knowledge can be leveraged to be a supervision signal. As shown in Figure 4, we train the one model to predict SBP, DBP and MBP in parallel. Note that such auxiliary training was only applied during training phase, and the model will not predict MBP in test stage. And we found that this multitask training strategy significantly improve the overall model accuracy performance comparing with the training individual model separately. It can be explained by that the different training objective involved in each task are strongly correlated and thus sharing a lot of data representations that capture the underlying factors, which can be learned by the same model structure (Caruana, 1998). By learning the shared representations, it can crucially improve the model generalization ability. On the other hand, multitask training also induced the regularization by requiring a model to perform well on multitask, namely penalizing overall complexity uniformly.

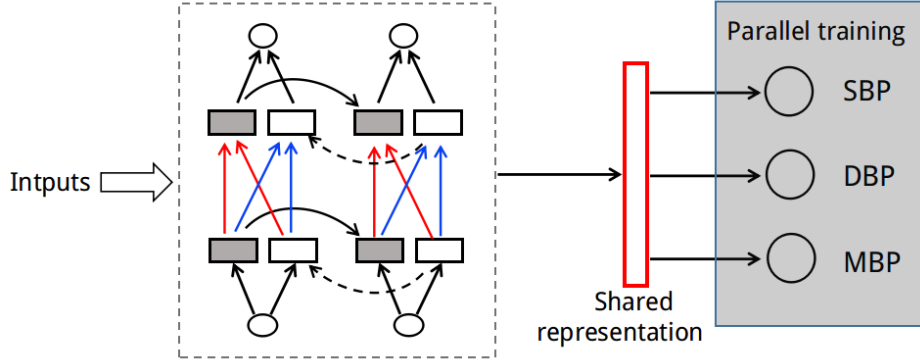


Figure 4: Multitask training pipeline. Training the model to predict SBP, DBP and MBP in parallel while using a shared data representation learned by lower hidden layers. And what is learned for each task can help other tasks to be learned better.

5.2 Supervised Pretraining

For follow-up continuous BP prediction task, we only have 8 subjects, each of which contain 8 minutes training samples at a day, and it is difficult to train a deep model like our DB-LSTM well on such a small dataset. Hence we first pretrained the model on the 62 subjects continuous BP dataset, and then finetuned the last output layer via backpropagation to perform follow-up continuous BP prediction task. Intriguingly, the experiment results show that even without finetuning on the follow-up dataset, the model trained on the 62 subjects dataset can perform slightly better than the model only trained the follow-up dataset.

6. Data Representation

In this section, we are going to investigate data representation details. The performance of machine learning methods is heavily depend on data representation, also known as features. For BP prediction problem, there have been extensive studies to discover or design new features to improve long-term BP prediction accuracy (Li et al., 2014; Ding and Zhang, 2014). Yet, there is no systematic study on which set of features are most effective to predict BP. Here we investigate the efficacy of data representation in detail. Through reviewing all features reported in literature, we obtain 16 features in total (Appendix A).³ We then apply Pearson correlation analysis and lasso feature selection method to remove either redundant or irrelevant features. Finally we select 11 features including PTT_s , HR , ST , STR , $SDTR$, $upTime$, RI , SV , DV , RSV and $SDVR$. During both training and testing stage, we extract 11 features above and then normalize them as inputs feeding into our DB-LSTM model.

3. Since our experiments only include ECG and PPG input data, here we only consider the features of ECG and PPG signal.

7. Experiments

We evaluate the proposed model on two tasks, static and follow-up continuous BP prediction. In both tasks we compare our model with several baseline models including :

- PTT model: we select two most cited PTT-based models - Chen’s method (Chen et al., 2000)⁴ and Poon’s method (Poon and Zhang, 2006).
- Typical regression models: support vector regression (SVR), decision tree (DT), and bayesian linear regression (BLR).
- Vanilla LSTM

In our experiment setup, mean absolute difference (MAD) between BP prediction and BP ground truth are used as the evaluation metrics. Here the unit of MAD is mmHg.

7.1 Dataset

Static continuous BP dataset. This dataset contains 62 healthy people with mean age of 26.7 ± 4.5 years (range from 21 to 42) including 36 males and 26 females. ECG and PPG signal were acquired by Biopac system and reference continuous BP was measured by Finapres system simultaneously in each experiment. The BP, ECG and PPG data of each subject was recorded for 10 minutes at the rest status.

Follow-up continuous BP dataset. This dataset contains 8 healthy subjects with mean age of 27.3 ± 4.5 years (from 22 to 33), including 7 males and 1 female. Similarly, ECG and PPG signals were acquired by Biopac system, with reference continuous BP by Finapres simultaneously during experiment procedure. The BP, ECG and PPG data of each subject was recorded for 8 minutes at the rest status in a follow-up period, namely 1st day, 2nd day, 4th day and 6 moth after the first day.

7.2 Training details

We trained our models using stochastic gradient descent with a batch size of 100 examples, momentum of 0.9, and weight decay of 0.0005. All of the LSTM’s parameters were initialized with the uniform distribution between -0.1 and 0.1. Although LSTM tend not to suffer from the vanishing gradient problem, they can have exploding gradients. Thus we clipped gradients at the threshold $v = 5$. For each minibatch, we computed the norm of gradients $\|g\|$. If $\|g\| > v$, the gradients were scaled by $gv/\|g\|$. We run our model with different number of layers, with 1024 cells at each layer. When the depth of our model exceed 2 layers, a dropout of 0.45 was applied at the following layers along depth direction. All the experiments of our models were implemented on a computer with a single NVIDIA GTX 1080 Ti GPU.

7.3 Experimental Results

For static continuous BP prediction task, the PTT models works slightly better than the regression models, but not as well as vanilla LSTM. By incorporating with a bidirectional

4. Chen’s PTT model only support SBP prediction, thus only its SBP prediction results were used to compare with other models.

Table 1: Comparison of MAD on static continuous BP prediction task.

Model	MAD(SBP)	MAD(DBP)
PTT-Chen(Chen et al., 2000)	8.23	-
PTT-Poon (Poon and Zhang, 2006)	8.24	4.32
SVR	9.79	6.78
DT	9.83	7.23
BLR	11.5	7.86
vanilla LSTM	7.56	5.78
bidirectional LSTM	5.31	4.1
DB-LSTM-2L	5.0	3.67
DB-LSTM-3L	4.13	2.8
DB-LSTM-4L	4.24	3.38

Table 2: Comparison of MAD on follow-up continuous BP prediction task. Model with an asterisk * was trained with multitask objective. See section 5.1 for details.

Model	MAD(SBP)				MAD(DBP)			
	1st day	2nd day	4th day	6th month	1st day	2nd day	4th day	6th month
PTT-Chen	5.0	8.28	10.12	11.4	-	-	-	-
PTT-Poon	6.7	10.1	11.5	12.73	4.36	7.12	8.17	9.02
BLR	7.45	10.59	10.61	11.20	7.45	6.38	7.06	7.74
SVR	7.94	9.90	11.18	11.59	7.94	6.92	7.68	7.59
DT	7.60	10.91	11.06	11.51	7.60	6.79	7.50	8.14
vanilla LSTM	6.3	8.25	8.2	8.27	4.0	5.8	6.5	6.48
bidirectional LSTM	5.14	7.9	8.16	8.21	3.9	5.13	6.45	6.9
DB-LSTM-3L	4.22	6.86	7.13	7.8	3.6	5.3	5.65	5.78
DB-LSTM-3L *	3.5	5.25	5.8	5.81	3.0	4.76	5.0	5.21

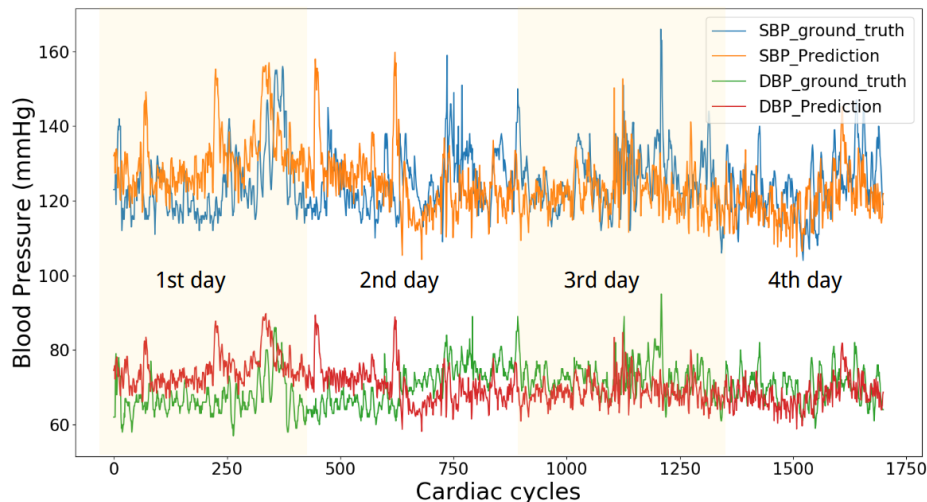


Figure 5: Comparison of the ground truth and DM-LSTM model prediction on a BP sequence of one representative subject. The result suggests that our DM-LSTM model can effectively learn the multi-timescale dependencies.

structure in the model, i.e. by using the bidirectional LSTM, the prediction accuracy has improved significantly as compared to the vanilla LSTM, with 29.8 % decrease in the SBP MAD and 29.1 % decrease in DBP MAD, as can be derived from Table 1. Furthermore, it was observed that increasing the depth of the DB-LSTM network can also improve the model’s prediction accuracy to different extent. For instance, a three-layer DB-LSTM model (DB-LSTM-3L) shows 22.2% and 31.7% improvements on SBP and DBP prediction respectively compared with one-layer DB-LSTM model. When we stack up to a 4-layer DB-LSTM, no clear benefits of depth can be observed any more.

Considering the computing efficiency and model performance, a 3-layer DB-LSTM network was selected for further comparison on the follow-up continuous BP prediction task. In this task, all models were trained using part of the first-day data and then tested on the rest of the first-day data as well as the following three-day’s data. All DB-LSTM models were pretrained on the static continuous BP dataset. Note that compared with static BP prediction, the multi-day BP prediction is generally much more challenging due to various random variations of human body and external environments. Typically, multi-day BP sequences have more intricate temporal dependence structure and larger variation range. As shown in Table 2, all the PTT models and regression models exhibit pronounced accuracy decay from the second day. Although the prediction accuracies of the DB-LSTM models also dropped over time, it consistently provides the lowest MAD values among all models. We also found that multitask training can further improve the performance of the DB-LSTM models by 21.2% on SBP and 12.1% on DBP (calculate by averaging on four different day). A 3-layers DM-LSTM trained by multitask achieved the best accuracy performance, as shown in Table 2. To qualitatively show the capability of the model to track BP variation, we plot the 4 day prediction results together with the ground truth (i.e. the reference BP values), as shown in Figure 5.

8. Conclusions and Future Work

In this work, we demonstrate for the first time that an RNN model is capable of learning the latent structures of different timescales in a long-term continuous BP sequence, which is the most tough challenge in predicting BP. We propose a new extension of LSTM called *deep bidirectional LSTM* (DB-LSTM) and combine with a multitask training strategy to tackle this challenge. The experimental results show that our DM-LSTM model can effectively capture the multiscale dependencies in the BP sequences and achieved the state-of-the-art accuracy performance on both on-day and follow-up continuous BP prediction tasks. In essence, we proposed a learning framework for BP sequence dependencies which can also be used to handle BP related classification tasks. The current model could be further developed to combine with feature extraction to build an end-to-end training model.

Acknowledgments

We thank Fen Miao and Ye Li from Key Laboratory for Health Informatics of the Chinese Academy of Sciences for providing the experiments data.

References

- Solange Akselrod, David Gordon, Jeffrey B Madwed, NC Snidman, DC Shannon, and RJ Cohen. Hemodynamic regulation: investigation by spectral analysis. *American Journal of Physiology-Heart and Circulatory Physiology*, 249(4):H867–H875, 1985.
- Yoshua Bengio, Aaron Courville, and Pascal Vincent. Representation learning: A review and new perspectives. *IEEE transactions on pattern analysis and machine intelligence*, 35(8):1798–1828, 2013.
- Rich Caruana. Multitask learning. In *Learning to learn*, pages 95–133. Springer, 1998.
- CH Chan, CCY Poon, Raymond CS Wong, and YT Zhang. A hybrid body sensor network for continuous and long-term measurement of arterial blood pressure. In *Medical Devices and Biosensors, 2007. ISSS-MDBS 2007. 4th IEEE/EMBS International Summer School and Symposium on*, pages 121–123. IEEE, 2007.
- Zhengping Che, Sanjay Purushotham, Kyunghyun Cho, David Sontag, and Yan Liu. Recurrent neural networks for multivariate time series with missing values. *arXiv preprint arXiv:1606.01865*, 2016.
- W Chen, T Kobayashi, S Ichikawa, Y Takeuchi, and T Togawa. Continuous estimation of systolic blood pressure using the pulse arrival time and intermittent calibration. *Medical and Biological Engineering and Computing*, 38(5):569–574, 2000.
- Edward Choi, Mohammad Taha Bahadori, and Jimeng Sun. Doctor ai: Predicting clinical events via recurrent neural networks. *arXiv preprint arXiv:1511.05942*, 2015.
- Edward Choi, Mohammad Taha Bahadori, Jimeng Sun, Joshua Kulas, Andy Schuetz, and Walter Stewart. Retain: An interpretable predictive model for healthcare using reverse

- time attention mechanism. In *Advances in Neural Information Processing Systems*, pages 3504–3512, 2016.
- XR Ding and YT Zhang. Photoplethysmogram intensity ratio: A potential indicator for improving the accuracy of ptt-based cuffless blood pressure estimation. In *Conference proceedings:... Annual International Conference of the IEEE Engineering in Medicine and Biology Society. IEEE Engineering in Medicine and Biology Society. Annual Conference*, volume 2015, pages 398–401, 2014.
- Jeffrey Donahue, Lisa Anne Hendricks, Sergio Guadarrama, Marcus Rohrbach, Subhashini Venugopalan, Kate Saenko, and Trevor Darrell. Long-term recurrent convolutional networks for visual recognition and description. In *Proceedings of the IEEE conference on computer vision and pattern recognition*, pages 2625–2634, 2015.
- Salah El Hihi and Yoshua Bengio. Hierarchical recurrent neural networks for long-term dependencies. In *Nips*, volume 409, 1995.
- Ian Goodfellow, Yoshua Bengio, and Aaron Courville. *Deep Learning*. MIT Press, 2016. <http://www.deeplearningbook.org>.
- Alex Graves, Abdel-rahman Mohamed, and Geoffrey Hinton. Speech recognition with deep recurrent neural networks. In *Acoustics, speech and signal processing (icassp), 2013 IEEE international conference on*, pages 6645–6649. IEEE, 2013.
- Arthur C Guyton, Thomas G Coleman, Allen W Cowley, Konrad W Scheel, R Davis Manning, and Roger A Norman. Arterial pressure regulation: overriding dominance of the kidneys in long-term regulation and in hypertension. *The American journal of medicine*, 52(5):584–594, 1972.
- Sepp Hochreiter and Jürgen Schmidhuber. Long short-term memory. *Neural computation*, 9(8):1735–1780, 1997.
- DJ Hughes, Charles F Babbs, LA Geddes, and JD Bourland. Measurements of young’s modulus of elasticity of the canine aorta with ultrasound. *Ultrasonic Imaging*, 1(4): 356–367, 1979.
- Mohamad Kachuee, Mohammad Mahdi Kiani, Hoda Mohammadzade, and Mahdi Shabany. Cuff-less high-accuracy calibration-free blood pressure estimation using pulse transit time. In *Circuits and Systems (ISCAS), 2015 IEEE International Symposium on*, pages 1006–1009. IEEE, 2015.
- Alex Krizhevsky, Ilya Sutskever, and Geoffrey E Hinton. Imagenet classification with deep convolutional neural networks. In *Advances in neural information processing systems*, pages 1097–1105, 2012.
- Yann LeCun, Yoshua Bengio, and Geoffrey Hinton. Deep learning. *Nature*, 521(7553): 436–444, 2015.

- Yanjun Li, Zengli Wang, Lin Zhang, Xianglin Yang, and Jinzhong Song. Characters available in photoplethysmogram for blood pressure estimation: beyond the pulse transit time. *Australasian Physical & Engineering Sciences in Medicine*, 37(2):367–376, 2014.
- Stephen S Lim, Theo Vos, Abraham D Flaxman, Goodarz Danaei, Kenji Shibuya, Heather Adair-Rohani, Mohammad A AlMazroa, Markus Amann, H Ross Anderson, Kathryn G Andrews, et al. A comparative risk assessment of burden of disease and injury attributable to 67 risk factors and risk factor clusters in 21 regions, 1990–2010: a systematic analysis for the global burden of disease study 2010. *The lancet*, 380(9859):2224–2260, 2013.
- Zachary C Lipton, David C Kale, Charles Elkan, and Randall Wetzell. Learning to diagnose with lstm recurrent neural networks. *arXiv preprint arXiv:1511.03677*, 2015.
- Zachary C Lipton, David C Kale, and Randall Wetzel. Directly modeling missing data in sequences with rnns: Improved classification of clinical time series. *arXiv preprint arXiv:1606.04130*, 2016.
- BM McCarthy, CJ Vaughan, B O’flynn, A Mathewson, and C Ó Mathúna. An examination of calibration intervals required for accurately tracking blood pressure using pulse transit time algorithms. *Journal of human hypertension*, 27(12):744–750, 2013.
- Tomas Mikolov, Martin Karafiát, Lukas Burget, Jan Cernocký, and Sanjeev Khudanpur. Recurrent neural network based language model. In *Interspeech*, volume 2, page 3, 2010.
- Enric Monte-Moreno. Non-invasive estimate of blood glucose and blood pressure from a photoplethysmograph by means of machine learning techniques. *Artificial Intelligence in Medicine*, 53(2):127–138, 2011.
- Wilmer Nichols, Michael O’Rourke, and Charalambos Vlachopoulos. *McDonald’s blood flow in arteries: theoretical, experimental and clinical principles*. CRC press, 2011.
- Gianfranco Parati, Paolo Castiglioni, Marco Di Rienzo, Stefano Omboni, Antonio Pedotti, and Giuseppe Mancia. Sequential spectral analysis of 24-hour blood pressure and pulse interval in humans. *Hypertension*, 16(4):414–421, 1990.
- Razvan Pascanu, Tomas Mikolov, and Yoshua Bengio. On the difficulty of training recurrent neural networks. *ICML (3)*, 28:1310–1318, 2013.
- CCY Poon and YT Zhang. Cuff-less and noninvasive measurements of arterial blood pressure by pulse transit time. In *2005 IEEE Engineering in Medicine and Biology 27th Annual Conference*, pages 5877–5880. IEEE, 2006.
- David E Rumelhart, Geoffrey E Hinton, and Ronald J Williams. Learning internal representations by error propagation. Technical report, DTIC Document, 1985.
- Mike Schuster and Kuldip K Paliwal. Bidirectional recurrent neural networks. *IEEE Transactions on Signal Processing*, 45(11):2673–2681, 1997.
- Rosaria Silipo and Carlo Marchesi. Artificial neural networks for automatic ecg analysis. *IEEE transactions on signal processing*, 46(5):1417–1425, 1998.

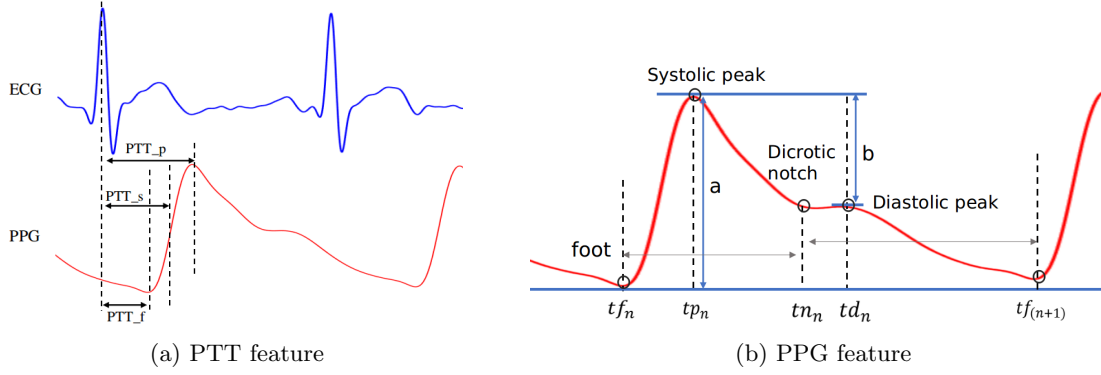


Figure 6: Features illustration.

Ilya Sutskever, James Martens, and Geoffrey E Hinton. Generating text with recurrent neural networks. In *Proceedings of the 28th International Conference on Machine Learning (ICML-11)*, pages 1017–1024, 2011.

Pierre Thodoroff, Joelle Pineau, and Andrew Lim. Learning robust features using deep learning for automatic seizure detection. *arXiv preprint arXiv:1608.00220*, 2016.

Oriol Vinyals, Alexander Toshev, Samy Bengio, and Dumitru Erhan. Show and tell: A neural image caption generator. In *Proceedings of the IEEE Conference on Computer Vision and Pattern Recognition*, pages 3156–3164, 2015.

Gershon Weltman, George Sullivan, and Dale Bredon. The continuous measurement of arterial pulse wave velocity. *Medical electronics and biological engineering*, 2(2):145–154, 1964.

Paul J Werbos. Generalization of backpropagation with application to a recurrent gas market model. *Neural networks*, 1(4):339–356, 1988.

Ya-Li Zheng, Xiao-Rong Ding, Carmen Chung Yan Poon, Benny Ping Lai Lo, Heye Zhang, Xiao-Lin Zhou, Guang-Zhong Yang, Ni Zhao, and Yuan-Ting Zhang. Unobtrusive sensing and wearable devices for health informatics. *IEEE Transactions on Biomedical Engineering*, 61(5):1538–1554, 2014.

Appendix A.

A. Data Representation

The total 16 features we extract in this paper are as follows:

- PTT_f : time interval from ECG R peak to the same heart cycle PPG foot (see Figure 6 a).
- PTT_S : time interval from ECG R peak to the same heart cycle PPG maximum slope.

- PTT_p time interval from ECG R peak to the same heart cycle PPG peak.
- Heart rate: HR
- Pulse interval: PI
- Reflection index: $RI = b/a$ (see Figure 6 b)
- Systolic timespan: $ST = tn_n - tf_n$
- Systolic diastolic timespan ration: $STR = \frac{tn_n - tf_n}{tf_{n+1} - tf_n}$
- Diastolic timespan ratio: $DTR = \frac{tf_{n+1} - tn_n}{tf_{n+1} - tf_n}$
- Systolic diastolic timespan ration: $SDTR = ST/DT$
- Up time: $upTime = tp_n - tf_n$
- Systolic volume: $SV = \int_{tf_n}^{tn_n} PPG(t)dt$
- Diastolic volume: $DV = \int_{tn_n}^{tf_{n+1}} PPG(t)dt$
- Relative systolic volume: $RSV = \frac{SV}{SV + DV}$
- Systolic diastolic volume ratio: $SDVR = SV/DV$
- Pulse wave velocity: $PWV = L/PTT_s$ (L is arm length.)

As Figure 7 shows, the elements in the feature subsets below are strong correlated, which indicate that there may be some redundant information among these features. This redundancy does not help the subsequent RNN model to learn but may harm the overall accuracy performance.

- PTT_f, PTT_s, PTT_p
- HR, PI
- STR, DTR
- PTT_f, PWV
- PTT_f, PTT_p, DV

Hence we use sparse methods to perform feature selection by inducing the model coefficient vector to be sparse. In other words, force the trivial feature's corresponding coefficient to be zero and thus can identify the most important features. Specifically, lasso method was applied to do feature selection and final 11 features were obtained as follows: $PTT_s, HR, ST, STR, SDTR, upTime, RI, SV, DV, RSV$ and $SDVR$.

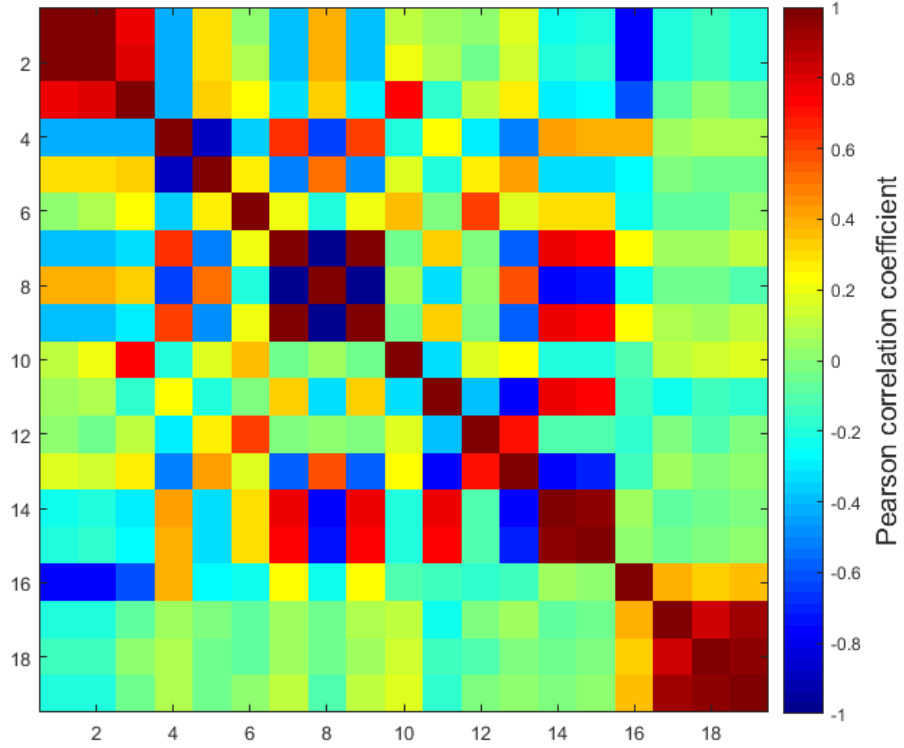


Figure 7: Features correlations analysis. The index from 1 to 19 indicate PTT_f , PTT_s , PTT_p , HR , PI , ST , STR , DTR , $SDTR$, $upTime$, RI , SV , DV , RSV , PWV , DBP , SBP and MBP respectively.